The $[C_6H_{10}]^{\bullet+}$ Hypersurface: the Parent Radical Cation Diels−Alder Reaction

Matthias Hofmann and Henry F. Schaefer III

Contribution from the Center for Computational Quantum Chemistry, University of Georgia, 1004 Cedar Street, Athens, GA, 30602-2525

Received September 18, 1998. Revised Manuscript Received May 16, 1999

Abstract: Various possible reaction pathways between ethene, **1**, and butadiene radical cation (*cis*-, **2**, *trans*-, **11**) have been investigated at different levels of theory up to UCCSD(T)/DZP//UMP2(fc)/DZP and with density functional theory at B3LYP/DZP. A stepwise addition involving open chain intermediates and leading to the Diels−Alder product, the cyclohexene radical cation, **6**, (path A) was found to have a total activation barrier $\Delta G^{298\neq} = 6.3$ kcal mol^{-1} and a change in free Gibbs energy, ΔG^{298}, of −33.5 kcal mol^{-1}. On the $E°$ potential energy surface, all transition states are lower in energy than separated **1** + **2**, the exothermicity $\Delta E = -45.6$ kcal mol^{-1}. A more direct path B could be characterized as stepwise with one intermediate only at the SCF level but not at electron-correlated levels and hence might actually be a concerted strongly asynchronous addition with a very small or no activation barrier (UCCSD(T)/DZP//UHF/6-31G* gives a $\Delta G^{298\neq}$ of 0.8 kcal mol^{-1}). The critical step for another alternative, the cyclobutanation−vinylcyclobutane/cyclohexene rearrangement, is a 1,3-alkyl shift which involves a barrier ($\Delta G^{298\neq}$) only 1.7 kcal mol^{-1} higher than that of path A for both *cis*-, **2**, (path C) and *trans*-butadiene radical cation, **11** (path D). However, from the **1** + **11** reactions, ring expansion of the vinylcyclobutane radical cation intermediate, **14**, to a methylene cyclopentane radical cation, **16**, (path E) requires an activation only 1.3 kcal mol^{-1} larger than for path D. While cis/trans isomerization of free butadiene radical cation requires a high activation (24.9 kcal mol^{-1}), a reaction sequence involving addition of ethene (to stepwise give an open chain intermediate **13** and vinyl cyclobutane radical cation, **10**) has a barrier of only 3.5 kcal mol^{-1} ($\Delta G^{298\neq}$). This sequence also makes ethene and butadiene radical cations to exchange terminal methylene groups.

Introduction

Pericyclic reactions are one of the most important reaction classes in organic synthesis as they allow transformations with high stereospecifity. However, there are also certain limitations: Some reactions may be prohibitively slow or proceed in a nondesired way. Lewis acids may assist as a catalyst by complexation, thereby reducing the electron density of one reactant. Alternatively, one electron may be removed from the system by an oxidizing agent or by photoinduced electron transfer (PET).[1] The more easily oxidizable reactant (if there is more than one) becomes a radical cation, which in contrast to the neutral molecule may readily react. If the product radical cation can be reduced by a reactant or by the reduced initiator molecule, the reaction bcomes a catalytic cycle. This electron-transfer approach has also been referred to as "hole catalysis" (Scheme 1).[2] The radical cation "pericyclic reactions" are a valuable complement to the neutral reactions, and there are a number of applications of synthetic interest.[3,4] The reactions generally have low activation energies but nevertheless show a high degree of peri-, regio-, and stereoselectivity.[4]

The Diels−Alder (DA) reaction,[5] a [4 + 2] cycloaddition used to build six-membered rings, is the most prominent representative of pericyclic reactions. However, in a neutral

Scheme 1

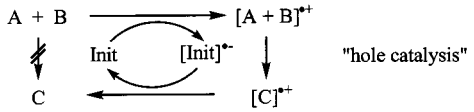

reaction, only some combinations of dienes and enes will react successfully: only if the HOMO and LUMO of the reactants are close enough in energy (frontier orbital concept).[6] Normally, only electron-rich dienes and electron-poor enes or, in an inverse reaction, electron-poor dienes and electron-rich enes will undergo an addition. Electron-transfer catalysis allows the addition of nonreactive compounds. This subject has been intensively investigated experimentally[4] since the catalytic effect of aminium radical cation salts on Diels−Alder reactions was observed in 1981 for the first time.[7] Consequently, Diels−Alder reactions also play an outstanding role among hole-catalyzed pericyclic reactions. Recent success stories include applications to ketenes,[8,9] indoles,[10] and electron-rich allenes.[11,12] Despite extensive experimental work there are several open questions concerning the mechanism. Reactions can be [3 + 2] (diene

(1) Müller, F.; Mattay, J. *Chem. Rev.* **1993**, *93*, 99.
(2) Bauld, N. L. *J. Am. Chem. Soc.* **1992**, *114*, 5800.
(3) Hintz, S.; Heidbreder, A.; Mattay, J. *Top. Curr. Chem.* **1996**, *177*, 77.
(4) For a review see: Bauld, N. L. *Tetrahedron* **1989**, *45*, 5307.
(5) Houk, K. N. *Acc. Chem. Res.* **1975**, *8*, 361.
(6) Fleming, I. *Frontier orbitals and organic chemical reactions*, Wiley: New York, 1977.
(7) Bellville, D. J.; Bauld, N. L. *J. Am. Chem. Soc.* **1981**, *103*, 718.
(8) Schmittel, M.; von Seggern, H. *Angew. Chem.* **1991**, *103*, 981.
(9) Schmittel, M.; von Seggern, H. *J. Am. Chem. Soc.* **1993**, *115*, 2165.
(10) (a) Gieseler, A.; Steckhan, E.; Wiest, O. *Synlett* **1990**, 275. (b) Wiest, O.; Steckhan, E.; Grein, F. *J. Org. Chem.* **1992**, *57*, 4034.
(11) (a) Schmittel, M.; Wöhrle, C. *Tetrahedron Lett.* **1993**, *34*, 8431. (b) Schmittel, M.; Wöhrle, C. *J. Org. Chem.* **1995**, *60*, 8223.
(12) Schmittel, M.; Wöhrle, C.; Bohn, I. *Chem. Eur. J.* **1996**, *2*, 1031.

10.1021/ja983338q CCC: $18.00
Published on Web 07/03/1999

radical cation plus ene) or [4 + 1] (diene plus ene radical cation) additions, and they can occur in a concerted or stepwise manner. The nature of transition states and intermediates must be understood to learn about the critical steps and possibilities for manipulating the reaction. While the Woodward−Hoffmann rules[13] and the frontier orbital concept[6] provide a basic understanding for neutral pericyclic reactions, even qualitative concepts are lacking for the radical cation reactions. Therefore more detailed insights into the mechanisms of these reactions are desirable. Experiments deal with highly substituted molecules, in most cases. Computations, however, are ideal to study the parent reactions and to reveal important intrinsic features.

The parent radical cation Diels−Alder reaction has already been considered theoretically. Assuming a true pericyclic process, Bellville and Bauld analyzed orbital correlation diagrams and classified the [4 + 1] cycloaddition (butadiene plus ethene radical cation) as symmetry-allowed and the [3 + 2] cycloaddition (butadiene radical cation plus ethene) to be symmetry-forbidden.[14] They conclude that the radical cation generally acts as dienophilic. Subsequent semiempirical MINDO/3 calculations characterized the reaction between *cis*-1,3-butadiene radical cation and ethene as concerted and highly nonsynchronous.[15] However, more recent experimental investigations indicate that the formally symmetry-forbidden [3 + 2] mechanism is a viable low-energy path[16,17] and best described as nonconcerted.[11]

The first ab initio treatment was reported in 1987.[18] On the basis of 6-31G*//3-21G computations, Bauld et al. conclude that the reaction is effectively activationless and concerted. Applying the MP3/6-31G*//SCF/3-21G method Bauld finds the cycloaddition to be concerted, nonsynchronous, and activationless in the gas phase with an estimated exothermicity of 38.0 kcal mol^{-1}.[2] A distonic[19] intermediate with an allylic cation and a terminal radical center (−12.2 kcal mol^{-1} vs separated reactants) was identified, but no transition structure for its formation was identified. The transition structure for the cyclization is only insignificantly (0.4 kcal mol^{-1}) higher, and from single-point energy calculations including electron correlation, it is even lower in energy (by 0.9 kcal mol^{-1}) than the intermediate. This clearly shows that a better theoretical treatment is needed, and the levels used are indeed known to be insufficient for the description of open shell species.[20] For the closely related hole-catalyzed ethylene dimerization, it has already been shown[21] that highly correlated levels significantly change the potential energy surface compared to the SCF treatment.[22]

The only experimental investigations of the parent reaction of ethene with butadiene radical cation are recent experiments conducted in a Fourier transform ion cyclotron resonance spectrometer with an external ion source.[23] However, under the low-pressure conditions no efficient deactivation of the adduct is possible and hence no $[C_6H_{10}]^{\bullet+}$ could be detected.

Derrick et al. investigated the reverse reaction, the dissociation of ionized cyclohexene into butadiene radical cation and ethene, by field ionization mass spectrometry.[24] By using 3,3,6,6-tetra deuterated cyclohexene, they found that this formally retro Diels−Alder reaction is preceded by hydrogen scrambling which was proposed to be a result of successive 1,3-allylic rearrangements. In addition to the butadiene radical cation (= $[M - C_2H_4]^{\bullet+}$), $[C_5H_7]^+$ (= $[M - [CH_3]^{\bullet}]^+$) and $[C_3H_5]^+$ (= $[M - [C_3H_5]^{\bullet}]^+$) were also detected.

We investigated the $[C_6H_{10}]^{\bullet+}$ potential energy hypersurface extensively applying modern high level ab initio (CCSD(T)/DZP//MP2/DZP) and density functional methods (B3LYP/DZP). The focus was on possible reaction pathways leading from the butadiene radical cation, $[C_4H_6]^{\bullet+}$, plus ethene, C_2H_4, to the cyclohexene radical cation, $[C_6H_{10}]^{\bullet+}$. Haberl et al. also studied the radical cation Diels−Alder reaction using similar methods (QCISD(T)/6-31G*//QCISD/6-31G* and B3LYP/ 6-31G*) and report similar results (relative energies of structures common to both papers are within 1 kcal mol^{-1}).[25]

Computational Details

All structures have been fully optimized at the UHF/3-21G, UHF/6-31G*, UMP2/6-31G*, UMP2/DZP, and B3LYP/DZP levels of theory in the specified symmetry point group using the Gaussian 94 program.[26] Important geometrical parameters at UMP2 and B3LYP/DZP are listed in Figures 1−5. Geometries discussed in the text correspond to UMP2(fc)/DZP unless stated otherwise. Plots including UHF/6-31G* and MP2(fc)/6-31G* data as well as Cartesian coordinates of UMP2(fc)/DZP optimized geometries are included as Supporting Information. Only valence electrons were considered in the MP2 electron correlation treatment ("frozen core" approximation). In addition to Pople's standard basis sets (3-21G, 6-31G*), a double ζ quality basis set of Huzinaga[27a] ("DZP") in the contraction scheme recommended by Dunning[27b] ((9s5p) contracted to [6111,41] for C and (4s) contracted to [31] for H) has been used together with one set of polarization functions (d type for C and p type on H with an exponent of 0.75 each). For density functional theory (DFT) treatment Becke's three parameter exchange functional[28] and the correlation functional of Lee, Yang, and Parr, which includes both local and nonlocal terms,[29] have been employed as implemented in Gaussian 94.[26,30] Because of the severe problems (discovered by Bally and Sastry[31]) of DFT methods in describing radical ion reactions where spin and charge are separated or brought together, DFT results should be treated with caution. Vibrational frequencies have been computed at all levels of optimization to determine the nature of the stationary points. Relative energies are corrected for scaled zero point vibrational energies (ZPE's) applying scaling factors of 0.89, 0.93, and 1.0 for UHF, UMP2, and UB3LYP, respectively. For UMP2(fc)/DZP geometries, single energy points have

(13) Woodward, R. B.; Hoffmann, R. *Angew. Chem.* **1969**, *81*, 797; *Angew. Chem., Int. Ed. Engl.* **1969**, *8*, 781.
(14) Bellville, D. J.; Bauld, N. L. *J. Am. Chem. Soc.* **1982**, *104*, 2665.
(15) Bauld, N. L.; Bellville, D. J.; Pabon, R.; Chelsky, R.; Green, G. *J. Am. Chem. Soc.* **1983**, *105*, 2378.
(16) Mlcoch, J.; Steckhan, E. *Tetrahedron Lett.* **1987**, *28*, 1081.
(17) Chokalingam, K.; Pinto, M.; Bauld, N. L. *J. Am. Chem. Soc.* **1990**, *112*, 447.
(18) Bauld, N.; Bellville, D. F.; Harirchian, B.; Lorenz, K.; Pabon, R. A.; Reynolds, D. W.; Wirth, D. D.; Chiou, H.-S.; Marsh, B. K. *Acc. Chem. Res.* **1987**, *20*, 371.
(19) A distonic radical cation has separated radical and cation centers.
(20) Clark, T. *Top. Curr. Chem.* **1996**, *177*, 1.
(21) (a) Jungwirth, P.; Cársky, P.; Bally, T. *J. Am. Chem. Soc.* **1993**, *115*, 5776. (b) Jungwirth, P.; Bally, T. *J. Am. Chem. Soc.* **1993**, *115*, 5783.
(22) Pabon, R. A.; Bauld, N. L. *J. Am. Chem. Soc.* **1984**, *106*, 1145.
(23) Bouchoux, G.; Salpin, J.-Y. *Rapid Commun. Mass Spectrom.* **1994**, *8*, 325.
(24) Derrick, P. J.; Fallick, A. M.; Burlingame, A. L. *J. Am. Chem. Soc.* **1972**, *94*, 6794.
(25) Haberl, U.; Wiest, O.; Steckhan, E. *J. Am. Chem. Soc.*, **1999**, *121*, 6730−6736.
(26) Frisch, M. J.; Trucks, G. W.; Schlegel, H. B.; Gill, P. M. W.; Johnson, B. G.; Robb, M. A.; Cheeseman, J. R.; Keith, T.; Petersson, G. A.; Montgomery, J. A.; Raghavachari, K.; Al-Laham, M. A.; Zakrzewski, V. G.; Ortiz, J. V.; Foresman, J. B.; Cioslowski, J.; Stefanov, B. B.; Nanayakkara, A.; Challacombe, M.; Peng, C. Y.; Ayala, P. Y.; Chen, W.; Wong, M. W.; Andres, J. L.; Replogle, E. S.; Gomperts, R.; Martin, R. L.; Fox, D. J.; Binkley, J. S.; Defrees, D. J.; Baker, J.; Stewart, J. P.; Head-Gordon, M.; Gonzalez, C.; Pople, J. A. *Gaussian 94*; Gaussian, Inc.; Pittsburgh, PA, 1995, Revision C.3.
(27) (a) Huzinaga, S. *J. Chem. Phys.* **1965**, *42*, 1293. (b) Dunning, T. H. *J. Chem. Phys.* **1970**, *53*, 2823.
(28) Becke, A. D. *J. Chem. Phys.* **1993**, *98*, 5648.
(29) Lee, C.; Yang, W.; Parr, R. G. *Phys. Rev. B: Solid State* **1988**, *37*, 785.
(30) Stephens, P. J.; Devlin, F. J.; Frisch, M. J. *J. Phys. Chem.* **1994**, *98*, 11623.
(31) Bally, T.; Sastry, G. N. *J. Phys. Chem. A* **1997**, *101*, 7923.

Table 1. Relative Energies[a] in Kilocalories per Mole for $[C_6H_{10}]^{\bullet+}$ Stationary Points Considered in This Study[b]

	1 + 2	**3**	**TS- 3/4**	**4**	**TS- 4/5**	**5**	**TS- 5/6**	**6**	**8**	**TS−8/9**	**9**	**TS-4/10**	**10**	**TS-6/10**
UMP2/DZP	52.2	44.8	48.1	38.4	39.4	40.9	44.8	0.0	43.8	46.7	40.7	43.1	28.0	45.3
(S^2)	(0.926)	(0.919)	(1.076)	(0.763)	(0.762)	(0.826)	(0.904)	(0.756)	(0.953)	(1.038)	(0.780)	(0.857)	(0.802)	(0.935)
ΔG^{298} correction[c]	*−12.1*	*−3.2*	*−2.7*	*−2.8*	*−1.7*	*−1.9*	*−1.1*	*0.0*	−2.0	−1.8	−2.7	−1.4	−0.9	−0.7
PMP2[d]	47.4	39.4	37.4	37.7	42.5	40.3	40.9	0.0	35.6	36.1	39.4	40.1	26.0	39.4
CCSD[d]	45.8	41.3	41.3	38.3	42.7	40.9	41.1	0.0	41.0	41.4	40.1	40.0	29.9	44.7
CCSD(T)[d]	45.6	39.0	38.9	36.9	41.5	39.7	39.3	0.0	39.4	38.8	38.2	38.4	28.2	42.2
ΔG^{298}[c]	33.5	35.8	36.2	34.1	39.8	37.8	38.2	0.0	37.4	37.0	35.6	37.0	27.3	41.5
//B3LYP/DZP	42.3	32.3	32.6	32.3	43.8	*f*	*f*	0.0				*g*	27.0	*f*
ΔG^{298} [e]	30.6	28.6	29.8	30.0	41.4	*f*	*f*	0.0				*g*	25.8	*f*

	TS-10/10	**1 + 11**	**12**	**TS−12/13**	**13**	**TS-13/14**	**14**	**TS-14/14**	**TS-10/14**	**TS-14/15**	**15**	**16**	**TS-16/17**	**17**
UMP2/DZP	31.7	48.0	40.9	44.1	36.1	39.7	27.4	29.2	34.2	34.5	26.7[i]	1.6	41.9	−8.9
(S^2)	(0.777)	(0.912)	(0.903)	(1.062)	(0.799)	(0.841)	(0.799)	(0.790)	(0.756)	(0.768)	(0.762)	(0.756)	(0.761)	(0.756)
ΔG^{298} correction[c]	−0.8	−12.0	−3.1	−2.5	−2.5	−1.2	−0.9	−0.7	−0.8	−0.6	−	−0.2	−0.2	−1.1
PMP2[d]	30.8	43.4	35.8	33.7	34.6	37.0	25.5	27.8	34.2	33.5	27.5[i]	1.6	41.4	−8.8
CCSD[d]	33.1	42.1	38.0	38.0	35.6	37.2	29.3	30.9	33.4	35.6	26.7[i]	1.9	45.3	−8.5
CCSD(T)[d]	31.4	42.0	35.8	35.7	33.8	35.6	27.8	29.2	32.8	34.1	26.4[i]	1.9	44.1	−8.7
ΔG^{298} [c]	30.6	30.0	32.7	33.2	31.3	34.4	26.9	28.5	32.0	33.5	24.6[i,j]	1.7	43.9	−9.8
//B3LYP/DZP	30.4	38.5	*f*	29.9	27.5	*h*	25.5	27.1	30.0	36.6	29.7[i]	2.9	49.2	−9.6
ΔG^{298} [e]	29.6	27.0	*f*	28.4	25.3	*h*	24.3	26.3	29.1	36.3	27.9[i,j]	2.7	49.0	−10.8

[a] Corrected for scaled zero point vibrational energies obtained at level of optimization. [b] See Figures 1−5 for the structures. [c] Thermal corrections at UMP2(fc)/DZP for T=298 K. [d] Using the DZP basis set and UMP2(fc)/DZP optimized geometries. [e] Thermal corrections at UB3LYP/DZP for T=298 K. [f] Attempts to localize the structure at UB3LYP/DZP were unsuccessful. [g] A transition-state search using the UMP2/DZP geometry as an input converged to a transition state for the C(6)H_2 rotation. [h] A transition-state search using the UMP2/DZP geometry as an input converged to a transition state for the C(6)H_2 rotation. [i] For UHF/6-31G* optimized geometry. [j] Thermal correction derived from UHF/6-31G* frequencies.

been computed at the coupled cluster level including single and double excitations with perturbative estimation of triple corrections and using the DZP basis set and a UHF reference wave function (UCCSD(T)/DZP).[32] Thermal corrections to free Gibbs energy values (ΔG^{298}) have been obtained from unscaled frequencies for a temperature of 298 K. Unless specified otherwise, relative energies ($\Delta E°$) reported in the text are obtained at the coupled cluster level (UCCSD(T)/DZP//UMP2(fc)/DZP + 0.93 ZPE(UMP2(fc)/DZP) for T = 0 K. These values have also been used in the sketches of the reaction paths A−E. At some points (mostly where entropy effects are important), ΔG^{298} energies are also discussed but this is explicitly stated in such circumstances. Energy values in Table 1 and in Charts 1−5 are given relative to the cyclohexene radical cation, which was chosen because of its very small spin contamination (S^2 = 0.756, ideal 0.750 for a doublet). While "spin-projected energies" (PMP2 in Table 1) and energies from CCSD(T) are not deteriorated much by spin-contaminated reference wave functions, (our UMP2 optimized) geometries may be affected. However, as spin expectation values (S^2) are much closer to that of a doublet (0.75) than that of a quartet (3.75) even in the worst cases (ca. 1.1 for some transition structures), we are hopeful that this is not a severe problem.

Results and Discussion

As *s-cis*-butadiene is more easily oxidizable than ethene, the ground-state reaction for the one electron oxidized system occurs between *cis*-butadiene radical cation and ethene. The separated *cis*-butadiene radical cation **1** and ethene **2** are computed to be 31.8 kcal mol^{-1} more stable than separated *s-cis*-butadiene and ethene radical cation. The initial step for a cyclization reaction between **1** and **2** is the formation of an ion−molecule complex. Such a complex, **3**, is stabilized by 6.6 kcal mol^{-1} vs its components, **1** and **2**, at 0 K but it has a 2.3 kcal mol^{-1} higher ΔG at 298 K (compare Table 1). In **3**, the ethene molecule is coordinated to one terminal carbon atom (C4) of the butadiene radical cation moiety. This contrasts the situation for the neutral molecules, which form a symmetric van der Waal complex as the precursor for the concerted Diels−Alder cycloaddition. This difference may be rationalized by considering the frontier orbitals. In the ethene/butadiene complex the C1−C6 and C4−C5 contacts are in phase in both the LUMO−HOMO and HOMO−LUMO interactions (Scheme 2). In the butadiene radical cation the SOMO is low in energy and its acceptor behavior dominates. As the SOMO has opposite phases on C1 and C4, the ethene HOMO can interact favorably with only one side (Scheme 2).

Scheme 2

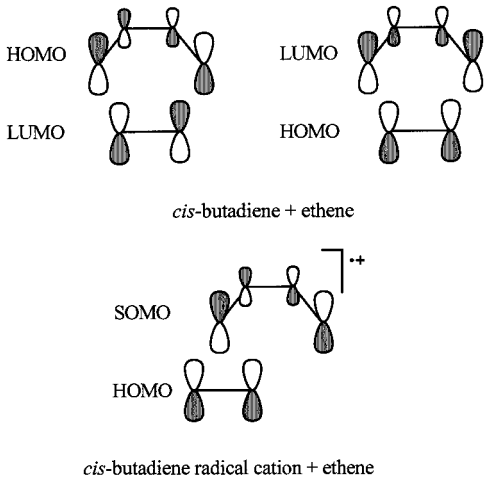

The intermolecular distances C4−C5 and C4−C6 between the butadiene and ethene units in **3** are similar: ∼2.60 Å (at the MP2 level; however, at B3LYP/DZP there is a pronounced difference of almost 0.3 Å, see Figure 1). Although the identities of the molecules are still conserved in **3**, there is a considerable interaction not only in terms of stabilization energy (6.6 kcal mol^{-1}) but also in terms of charge and spin transfer. There is a net charge transfer of 0.23 electrons from the ethene to the butadiene unit in **3** according to a natural population analysis (NPA)[33]). The ethene molecule seems to polarize the alpha spin density away from C4, and the spin density values at C1, C2, and C3 (0.814, −0.481, 0.453) are more reminiscent of the allyl radical (0.979, −0.726, 0.979) than of butadiene radical cation (0.712, −0.117, −0.117).

(32) (a) Purvis, G. D.; Bartlett, R. J. *J. Chem. Phys.* **1982**, *76*, 1910. (b) Rittby, M.; Bartlett, R. J. *J. Phys. Chem.* **1988**, *92*, 3033.

(33) Reed, A. E.; Weinhold, F. *Chem. Rev.* **1988**, *88*, 899.

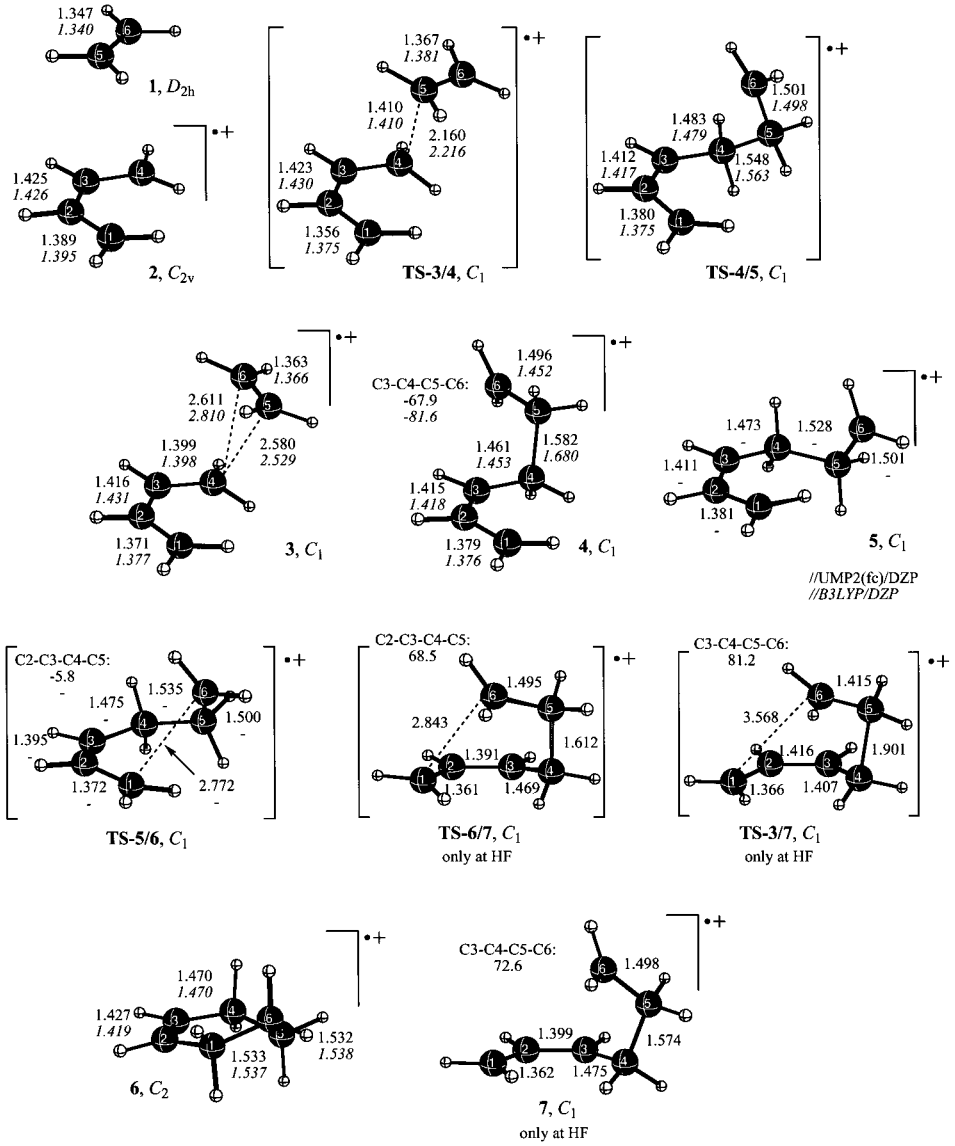

Figure 1. Optimized geometries for ethene, **1**, the *cis*-butadiene radical cation, **2**, and various stationary points for the cyclization reaction leading to the cyclohexene radical cation, **6**.

Bellville and Bauld described a computed "π complex",[34] but Bauld reported later that only a "σ complex" could be confirmed as an energy minimum.[2] In the latter, however, the ethene carbon atoms lie in the molecular plane of the butadiene radical cation while the ethene CH bonds are perpendicular to it. Such an arrangement, however, seems not suitable for an addition reaction, and consequently, no direct route to the Diels−Alder reaction could be found by Bellville and Bauld.

Carbon atom C4 of the butadiene radical cation moiety in **3** can form a bond to either carbon atom of ethene. Both ways will be discussed in detail subsequently (but the ethene carbon atom attached to C4 will be labeled C5 in each case).

I. Path A: Stepwise Indirect Addition. Ethene can add to the *cis*-butadiene radical cation forming a C−C bond with a terminal carbon atom (C4) while its other carbon atom (C6) points away from the C1 terminal butadiene carbon. Such an intermediate, **4**, is a distonic[19] radical cation with a C1−C2−C3 allyl cation moiety and a terminal radical center at C6.[35] This description is justified by large charges on C1 and C3 (0.48 and 0.54) and large positive spin density on C6 (1.21, compare Table 2). The barrier between **3** and **4** is 3.3 kcal mol^{-1} at our highest level of geometry optimization (MP2(fc)/DZP). At our final CCSD(T)/DZP level the energy of the transition structure **TS-3/4** becomes 0.1 kcal mol^{-1} more stable than **3** (Table 1). In conclusion, adding an ene to a diene radical cation seems to be an extremely facile process. On the ΔG^{298} surface (CCSD(T)/DZP//UMP2(fc)/DZP including thermal corrections from MP2/DZP frequencies), the barrier is only 0.4 kcal mol^{-1} relative to **3** and 2.7 kcal mol^{-1} vs separated **1** + **2** (Table 1).

Rotation around the C3−C4 bond transforms **4** into conformer **5** with C1 to C5 in a quasi planar arrangement (C1−C2−C3−C4 = 11.5°, C2−C3−C4−C5 = −3.5°) and the radical center at C6 favorably oriented relative to C1 for ring closure. The

(34) Bellville, D. J.; Bauld, N. L *Tetrahedron* **1986**, *42*, 6167.

(35) A preference for a C1−C2−C3 allyl cation moiety plus a C6 radical center over the C1−C2−C3 allyl radical plus C6 cationic center alternative can be expected from the −48.9 kcal mol^{-1} energy difference (CCSD(T)/DZP//UMP2(fc)/DZP + 0.93 ZPE(UMP2(fc)/DZP)) for the following reaction: allyl radical + methyl cation → allyl cation + methyl radical. Attempts to optimize the geometry for an open chain distonic radical cation with a primary carbocation center at C6 and a C1−C2−C3 allylic moiety resulted in a proton moving from C5 to C6.

Table 2. NPA Charges and Spin Densities (Italics) Computed at the UHF/DZP//UMP2(fc)/DZP Level of Theory (unless Stated Otherwise) for $[C_6H_{10}]^{\bullet+}$ Stationary Points

	C1	C2	C3	C4	C5	C6		C1	C2	C3	C4	C5	C6
1 + 2	0.358	0.142	0.142	0.358	0.0	0.0	**TS-6/10**	0.282	−0.063	0.408	0.038	0.070	0.265
	0.712	*−0.117*	*−0.117*	*0.712*	*0.0*	*0.0*		*1.125*	*−0.159*	*0.248*	*−0.034*	*0.017*	*−0.083*
3	0.215	0.054	0.111	0.390	0.099	0.131	**TS-10/10**	0.326	0.378	−0.100	0.165	0.065	0.165
	0.814	*−0.481*	*0.453*	*0.208*	*0.112*	*0.075*		*0.804*	*0.143*	*−0.044*	*0.124*	*−0.021*	*0.124*
TS-3/4	0.167	0.004	0.137	0.278	0.160	0.255	**1 + 11**	0.377	0.123	0.123	0.377	0.00	0.00
	0.799	*−0.589*	*0.629*	*−0.759*	*−0.240*	*0.665*		*0.709*	*−0.119*	*−0.119*	*0.709*	*0.000*	*0.000*
4	0.483	−0.155	0.544	0.008	0.042	0.078	**12**	0.257	0.027	0.111	0.384	0.101	0.121
	−0.026	*0.010*	*0.031*	*0.027*	*−0.142*	*1.214*		*0.785*	*−0.438*	*0.389*	*0.247*	*0.101*	*0.087*
TS-4/5	0.497	−0.162	0.553	0.029	0.009	0.073	**TS-12/13**	0.213	−0.020	0.137	0.272	0.155	0.243
	−0.011	*0.007*	*0.005*	*0.016*	*−0.138*	*1.213*		*−0.759*	*−0.528*	*0.542*	*−0.022*	*−0.287*	*0.720*
5	0.508	−0.170	0.532	0.060	0.002	0.067	**13**	0.422	−0.105	0.503	0.023	0.034	0.123
	0.269	*−0.084*	*−0.159*	*0.032*	*−0.145*	*1.203*		*0.179*	*−0.090*	*−0.026*	*0.070*	*−0.171*	*1.208*
TS-5/6	0.496	−0.149	0.508	0.057	0.004	0.083	**TS-13/14**	0.400	−0.096	0.477	0.039	0.054	0.126
	−0.341	*0.092*	*0.292*	*−0.021*	*−0.135*	*1.159*		*0.358*	*−0.169*	*−0.075*	*0.040*	*−0.127*	*1.075*
6	0.048	0.390	0.390	0.048	0.062	0.062	**14**	0.295	0.289	0.029	0.094	0.069	0.224
	0.009	*0.549*	*0.549*	*0.009*	*−0.079*	*−0.079*		*0.866*	*−0.035*	*0.047*	*0.006*	*−0.007*	*0.229*
TS-6/7[a]	0.408	−0.042	0.428	0.019	0.044	0.144	**TS-14/14**	0.343	0.325	−0.095	0.182	0.064	0.182
	−0.298	*−0.004*	*0.474*	*−0.025*	*0.101*	*1.065*		*0.791*	*0.0838*	*−0.040*	*0.153*	*−0.032*	*0.153*
7[a]	0.491	−0.158	0.538	0.009	0.044	0.076	**TS-10/14**	0.382	0.466	−0.055	0.056	0.084	0.067
	−0.279	*0.086*	*0.203*	*0.024*	*−0.131*	*1.219*		*0.754*	*0.368*	*−0.079*	*0.033*	*0.003*	*0.022*
TS-3/7[a]	0.237	−0.035	0.270	0.142	0.144	0.242	**TS-10/14***[a]	0.171	−0.098	0.382	0.081	0.085	0.379
	0.693	*−0.497*	*0.408*	*0.005*	*−0.296*	*0.924*		*0.232*	*−0.268*	*0.510*	*−0.015*	*−0.026*	*0.585*
8	0.084	0.000	0.038	0.193	0.303	0.381	**TS-14/15**	0.144	−0.092	0.616	0.055	0.077	0.200
	0.963	*−0.693*	*0.920*	*−0.117*	*0.024*	*0.073*		*1.189*	*−0.160*	*0.102*	*−0.014*	*0.006*	*0.055*
TS-8/9	0.113	−0.009	0.108	0.182	0.151	0.454	**15**[a]	0.140	−0.082	0.720	0.056	0.084	0.082
	0.873	*−0.661*	*0.812*	*−0.187*	*−0.125*	*0.472*		*1.226*	*−0.144*	*0.037*	*0.002*	*0.002*	*0.022*
9	0.405	−0.109	0.533	0.013	0.036	0.122	**16**	0.328	0.426	0.044	0.079	0.079	0.044
	0.148	*−0.082*	*−0.009*	*0.060*	*−0.165*	*1.212*		*0.822*	*0.306*	*−0.044*	*0.004*	*0.004*	*−0.044*
10	0.285	0.290	0.044	0.069	0.099	0.212	**17**	0.103	0.375	0.587	0.013	0.129	−0.207
	0.864	*−0.364*	*0.044*	*0.008*	*0.004*	*0.237*		*−0.047*	*0.415*	*0.663*	*−0.109*	*0.024*	*−0.077*
TS-4/10	0.406	−0.116	0.523	0.022	0.053	0.111	**TS-16/17**[b]	0.154	0.337	0.327	0.072	0.086	0.023
	0.380	*−0.191*	*−0.091*	*0.045*	*−0.131*	*1.108*		*−0.107*	*−0.119*	*0.029*	*0.027*	*−0.070*	*1.071*

[a] UHF/DZP//UHF/6-31G*. [b] The charge of the migrating H was distributed equally between C1 and C3.

transition structure **TS-4/5** involved has a 4.6 kcal mol^{-1} barrier. The fact that conformer **5** is (2.8 kcal mol^{-1}) less stable than **4** can be explained by hyperconjugation effects. The C4−C5 bond in **4** is favorably oriented to effectively hyperconjugate with the C1−C2−C3 allyl cation moiety. In **5** the C4−C5 bond lies approximately in the C1−C2−C3 plane and HC groups are not as effective donors as CC bonds. The geometric effects of the hyperconjugation are elongation of the C4−C5 bond, shortening of the C3−C4 distance (compare **4** to **5** in Figure 1), and a small C3−C4−C5 angle (107° in **4** vs 123.7° in **5**).

The final step of cyclization to give **6** involves bond formation between C1 and C6. It is exothermic by 39.7 kcal mol^{-1} with a very small barrier (vanishing at UCCSD(T)). The C1−C6 separation in transition structure **TS-5/6** is still very long (2.77 Å, in **5** it is 3.23 Å), and the other geometric parameters are quite similar to those of **5**. This is in line with Hammond's postulate that transition states of strongly exothermic reactions fall early on the reaction coordinate and are very reactant-like. While the radical center is still located at C6, negative spin density is shifted within the allylic moiety toward C1 for the bond formation.

Like minimum **5**, we were able to locate transition-state **TS-5/6** only at UHF and UMP2, but not at the UB3LYP level. In an important recent paper, Bally and Sastry showed that modern DFT functionals such as B3LYP (and BLYP and BHandH) are unable to describe transition states involving localization or separation of spin and charge in radical ions.[31] For the model systems $[H_2]^{\bullet+}$ and $[He_2]^{\bullet+}$ they demonstrated that DFT methods give qualitatively incorrect dissociation curves and that spin and charge are described as delocalized between the fragments even at very large distances. Another problem is that Kohn−Sham solutions of localized charge and spin may be found that are higher in energy than the delocalized solution, a phenomenon that has been called "inverse symmetry breaking". While we localized most of the $[C_6H_{10}]^{\bullet+}$ minima also at B3LYP/DZP, we were unable to find some of the transition states which bring spin and charge together. Methods, however, that cannot map the whole potential energy surface are of limited use. For minima we also note a tendency of DFT to distribute spin and charge more equally as compared to HF results. For example, for **4** we find (B3LYP/DZP) spin densities of 0.26, 0.22, and 0.74 at C1, C3, and C6, respectively, as compared to −0.03, 0.03, and 1.21 at HF/DZP//MP2/DZP. The DFT computed charge on C6 on the other hand is larger (0.29 vs 0.08 at HF).

At 0 K in the gas phase the relative energies of all intermediates and transition structures are well below the separated reactants, **1** and **2** (compare CCSD(T) values in Table 1 and Chart 1). At 298 K, however, entropy effects favor separated **1** + **2** much more than all of the intermediates. The rotation transition structure **TS-4/5** determines the effective barrier of 6.3 kcal mol^{-1} for the **1** + **2** → **6** addition on the ΔG^{298} hypersurface.

Haberl et al. report a more direct stepwise "anti pathway"[25] than path A (compare Chart 1). Rotation about the C4−C5 bond transforms the primary distonic adduct intermediate into the cyclohexene radical cation through a transition structure that is lower in energy than that for the ethene to butadiene radical cation addition and without further intermediates.[25] Its relative energy is 38.8 kcal mol^{-1} at our CCSD(T)/DZP//UMP2/DZP + ZPE level.

II. Path B: Direct Addition. As an alternative to path A, ethene can add to *s-cis*-butadiene, forming one C−C bond (C4−C5) while the terminal radical center (C6) is oriented toward

Chart 1

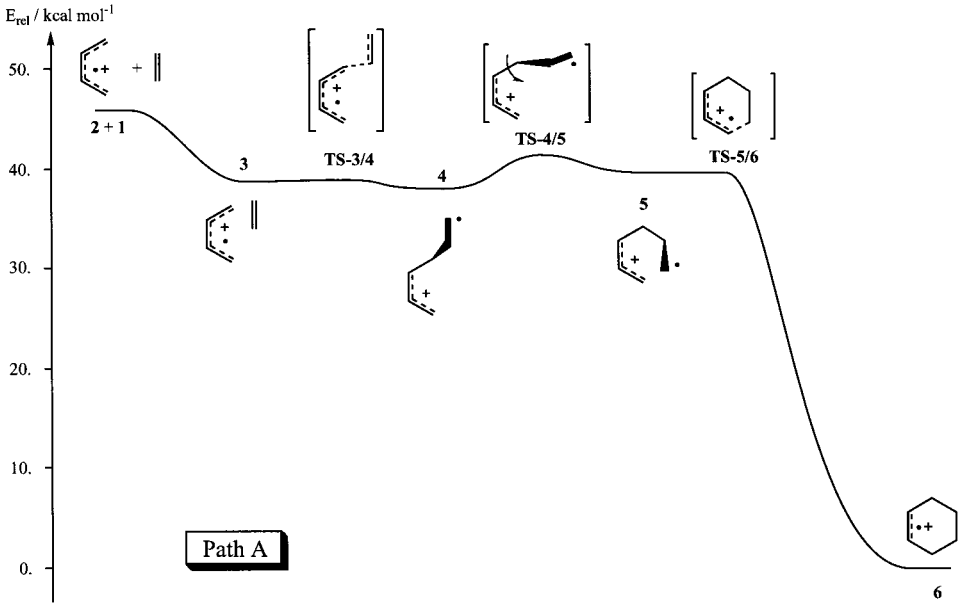

Chart 2

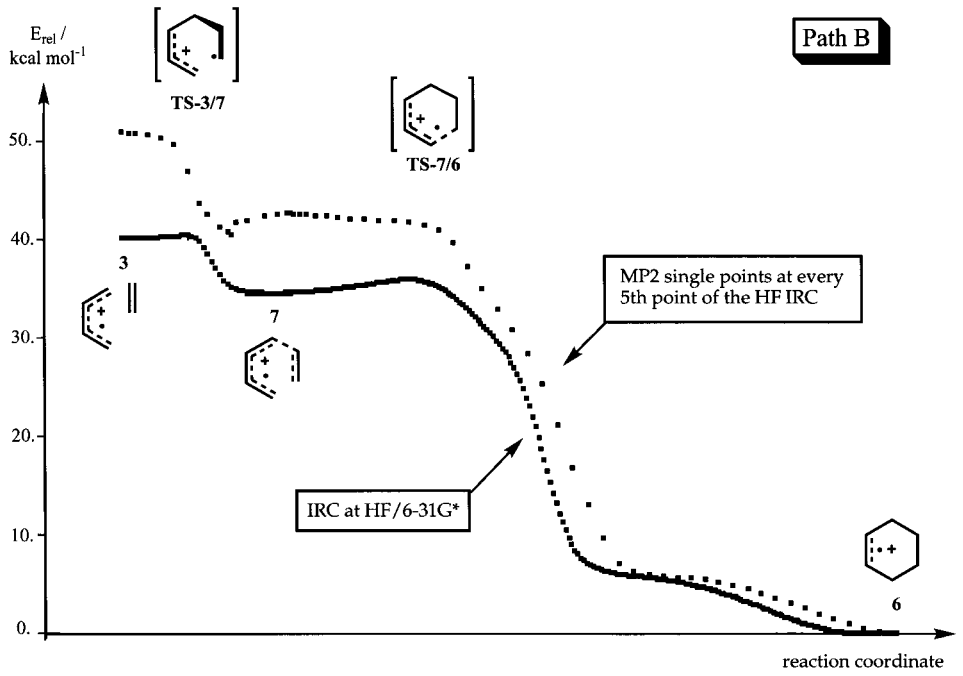

the C1−C2−C3 allyl moiety (in contrast to intermediate **4** where C6 is oriented away from the allyl). The resulting structure, **7**, was already found by Bauld at the UHF/3-21G level[2] and was located by us on the UHF/6-31G* potential energy surface, where it is 1.8 kcal mol^{-1} lower in energy than **3**. In addition, we were able to locate **TS-3/7**, the transition structure connecting **3** and **7**, at UHF/6-31G*. In this case, the barrier for the first bond formation is 3.5 kcal mol^{-1}, while it is slightly higher (4.2 kcal mol^{-1}) for path A (**TS-3/4** vs **3**) at the same level (i.e., UHF/6-31G*).

The transition state (**TS-6/7**) for C1−C6 ring closure in **7** to give **6** is again early (as **TS-5/6**). The barrier is 2.5 kcal mol^{-1} for this 31.1 kcal mol^{-1} (UHF/6-31G*) exothermic step (from **7** to **6**). Intrinsic Reaction Coordinates (IRC's) starting at **TS-3/7** and at **TS-6/7** confirmed the connection to the described minima (Chart 2). However we were unsuccessful in locating path B at MP2 or B3LYP. "Refining" the UHF optimized geometry of **7** at these levels directly converged to **6**. A transition-state search starting with the SCF structure of **TS-3/7** converged to **TS-8/9** which we found to connect **8** and **9** (Figure 2) by following the intrinsic reaction coordinate (IRC calculation) at the MP2(fc)/6-31G* level.

We also computed MP2(fc)/6-31G* single points for every fifth point of the UHF/6-31G* IRC in order to get an idea where to look for a transition state or minima between **3** and **6**. The energy decreases steadily between **7** and **6**, and it also decreases starting at **3** well beyond **TS-3/7**. However, there is a discontinuity between **TS-3/7** and **7** (compare Chart 2). This is because the method applied does not describe a real IRC but only the projection of the UHF IRC onto the MP2 potential hypersurface. MP2(fc)/6-31G* optimization of a starting geometry corresponding to the discontinuity point again converged to **6**. Single-point calculations at correlated levels (MP2, CCSD, and CCSD(T)) for the UHF/6-31G* optimized structures of **1** + **2**,

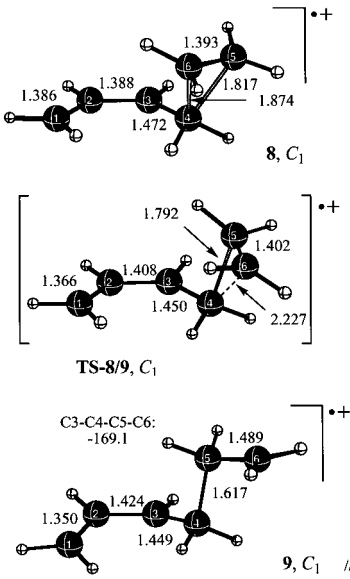

Figure 2. Optimized geometries of **8** and **9** and the transition state **TS-8/9**.

Table 3. Relative Energies[a] in Kilocalories per Mole of Path B Stationary Points at UHF/6-31G* Optimized Geometries (see Figure 1)

	1 + 2	**3**	**TS-3/7**	**7**	**TS-6/7**	**6**
UHF/6-31G*	35.6	32.9	36.4	31.1	33.6	0.0
(S^2)	(0.931)	(0.922)	(1.104)	(0.858)	(0.94)	(0.755)
ΔG^{298} correction[b]	*−12.3*	*−6.5*	*−2.3*	*−3.0*	*−1.0*	*0.0*
UHF/DZP	35.9	33.8	37.6	31.4	34.5	0.0
(S^2)	(0.925)	(0.916)	(1.098)	(0.840)	(0.931)	(0.756)
UMP2/DZP	52.4	47.0	43.0	38.7	34.5	0.0
PMP2/DZP	49.0	43.7	34.2	37.6	37.0	0.0
CCSD	46.4	42.0	38.1	36.5	33.5	0.0
CCSD(T)	46.3	41.3	35.3	35.0	30.9	0.0
ΔG^{298} [b]	34.0	34.8	33.0	32.0	29.8	0.0
B3LYP	41.6	33.7	30.2	31.2	27.5	0.0

[a] Including scaled (0.89) zero-point vibrational energies obtained at UHF/6-31G*. [b] Thermal corrections at UHF/6-31G* for $T = 298$ K.

3, **TS-3/7**, **7**, **TS-7/6**, and **6** suggest that there is a steady decrease of the relative energy along path B (Table 3). ΔG^{298} estimations from CCSD(T)/DZP//UHF/6-31G* single points and thermal corrections from UHF/6-31G* vibrational frequency calculations give a small 0.8 kcal mol^{-1} barrier for the formation of complex **3** with no further barrier to cyclization. Although methods applicable today are not able to give a definite answer, it seems that path B may consist of a concerted strongly asynchronous reaction from **1** + **2** to **6** with a very small or no activation energy at higher levels of theory.

The overall exothermicity (at 0 K) for the reaction **1** + **2** → **6** is predicted to be 45.6 kcal mol^{-1} here, compared to Bauld's estimation of 38.0 kcal mol^{-1}. For the change in free Gibbs energy (ΔG^{298}) we compute 33.5 kcal mol^{-1}.

III. Path C: Cyclobutanation/Vinylcyclobutane−Cyclohexene Rearrangement. We have also traced another alternative, namely the indirect cyclobutanation/vinylcyclobutane−cyclohexene rearrangement route. The neutral [2 + 2] addition of ethene to one double bond of butadiene gives vinylcyclobutane, and the subsequent 1,3-alkyl shift leads to ring expansion to give the overall Diels−Alder product, cyclohexene (Scheme 3). For the neutral reaction the initial addition step is a forbidden process (which means it should have a high barrier), and for the vinylcyclobutane to cyclohexene rearrangement (also forbidden) a large activation barrier of 48.6(4) kcal mol^{-1} has been

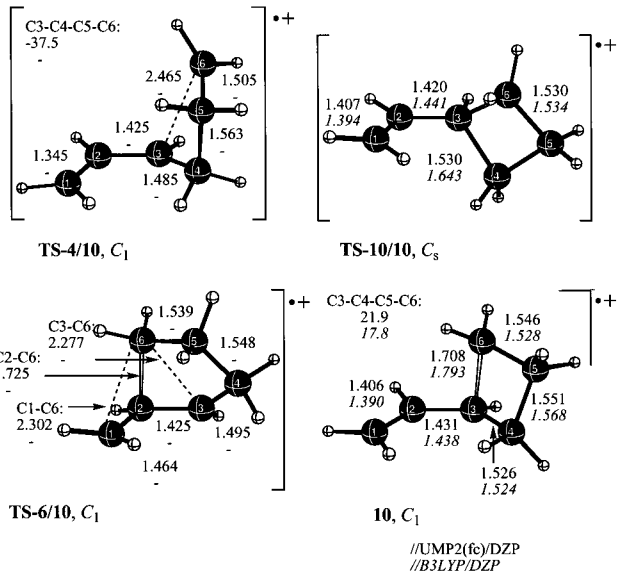

Figure 3. Optimized $[C_6H_{10}]^{\bullet+}$ geometries for stationary points of the hole-catalyzed cyclobutanation/vinylcyclobutane rearrangement mechanism (path C).

Scheme 3

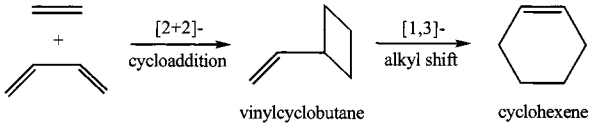

determined experimentally.[36] For the radical cation reaction, however, cyclobutanation has been demonstrated to be a useful synthetic reaction. Together with the vinylcyclobutane rearrangement it provides an effective method for net Diels−Alder additions.[4,37] It has been shown[38] that direct and indirect mechanisms can be competitive (e.g., hole-catalyzed addition of phenyl vinylsulfide to 1,1′-bicyclopentenyl).

While we could not locate a transition structure for a concerted [2 + 1] addition of ethene **1** to *cis*-butadiene radical cation **2**, we find a stepwise cyclobutanation. Rotation around the C4−C5 bond in **4** (decreasing the absolute value of the C3−C4−C5−C6 dihedral angle) brings the C6 radical center close to C3 of the C1−C2−C3 allyl cation moiety. The barrier for the combined C−C rotation and formation of a four-membered ring via transition structure **TS-4/10** to give the vinyl cyclobutane radical cation **10** is only 1.5 kcal mol^{-1}. Due to the additional bonding interaction, **10** is 8.7 kcal mol^{-1} more stable than **4**. Bauld[39] reported an optimized geometry (using the 3-21G basis set) for **10** with a long C3−C6 distance of 1.966 Å.[40] Electron correlation, however, considerably shortens the C3−C6 bond to ∼1.71 Å. In **10**, the C3−C6, C1−C2, and C2−C3 distances are 1.708, 1.406, and 1.431 Å, respectively, and the C2−C3−C6 angle is 97.7° (Figure 3). Corresponding values in 1-butene radical cation in a conformation that allows the C3−C4 bond to hyperconjugate with the oxidized C1−C2 π-bond

(36) Frey, H. M.; Pottinger, R. *J. Chem. Soc., Faraday Trans. 1* **1978**, 1827.

(37) Reynolds, D. W.; Harirchian, B.; Chiou, H.-S.; Marsh, B. K.; Bauld, N. L. *J. Phys. Org. Chem.* **1989**, *2*, 57.

(38) Kim, T.; Pye, R. J.; Bauld, N. L. *J. Am. Chem. Soc.* **1990**, *112*, 6285.

(39) Bauld, N. L. *J. Comput. Chem.* **1990**, *11*, 896.

(40) While we were able to reproduce the data on **7** at UHF/3-21G, our results differ from the geometric parameters and the absolute energies reported for **10** and **TS-6/10** in ref 39. The method and programs used in that work were not described fully.

Scheme 4

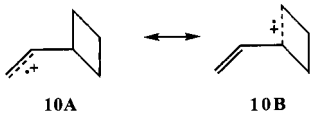

Chart 3

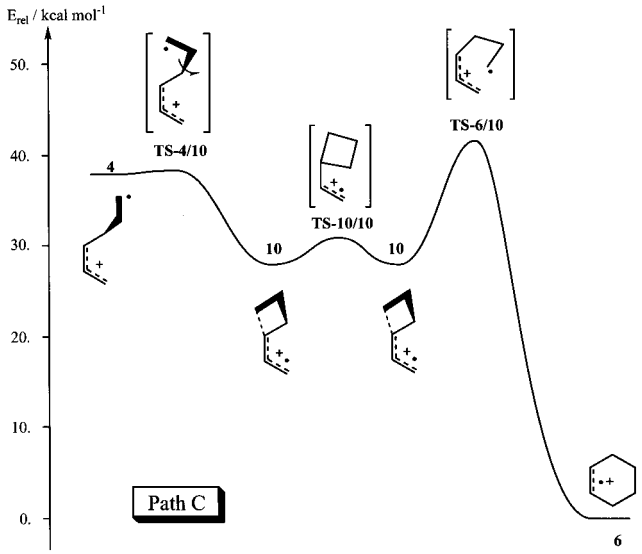

are 1.595 Å, 1.422 Å, 1.450 Å and 102.8°, respectively. Obviously, the strained cyclobutyl C−C bond (C3−C6 in **10**) undergoes a stronger hyperconjugative interaction. Intermediate **10** may be described by two resonance structures: in **10A** the C1−C2 double bond has lost one electron while in **10B** the electron is missing from the C4−C6 single bond (Scheme 4). This may be viewed as a 4-center 3-electron bonding situation.

The 1,3-alkyl shift for the rearrangement of **10** into **6** is not as facile as the formation of **10**, however. The barrier is 14.0 kcal mol^{-1} which is somewhat higher than Bauld's 9.4 kcal mol^{-1} estimation[39] but still much less than the (experimentally determined) 48.6(4) kcal mol^{-1} for the corresponding neutral rearrangement of vinylcyclobutane to cyclohexene.[36] Bauld described the transition state responsible for the estimated effective 9.4 kcal mol^{-1} barrier for the rearrangement of **10** to cyclohexene radical cation, **6**, as connecting **10** and **7**. However, we computed an IRC and found that **TS-6/10** really connects **6** and **10** directly, without any intermediate between (see Chart 3). Transition-state **TS-6/10** is somewhat higher in energy than the transition state for ring opening, **TS-4/10**, (by 4.5 kcal mol^{-1} on ΔG^{298}) and the highest transition structure for the stepwise addition (Path A), **TS-4/5** (by 1.7 kcal mol^{-1} on ΔG^{298}). The spin density on C6 in **TS-6/10** is 1.108, while the charges at C1, C2, and C3 are 0.28, −0.06, and 0.41. These suggest a description of a radical center at C6 moving over an allylic cation moiety.

The degenerate rearrangement which interchanges C4 and C6 through the C_s-symmetric transition state, **TS-10/10**, has a barrier of only 3.2 kcal mol^{-1}. This is considerably less than the barriers for formation of **10** (7.0 kcal mol^{-1}) and for ring expansion of **10** (10.8 kcal mol^{-1}). Hence, exchange of terminal CH_2 groups between **1** and **2** as observed experimentally by Bouchoux and Salpin can occur very easily through the formation of **10**.

IV. Path D: Cyclobutanation/Vinylcyclobutane−Cyclohexene Rearrangement with *trans*-Butadiene Radical Cation. For stereoelectronic reasons, *s-trans*-butadiene cannot add an ene in a neutral concerted [4 + 2] cycloaddition. But as the radical cation reaction can proceed in a stepwise manner with low activation energy (as shown above), the question arises whether the diene component really has to be in its *s-cis*-conformation for a hole-catalyzed Diels−Alder reaction. The *s-trans*-butadiene is more stable than its s-cis isomer by 2.7 kcal mol^{-1}, and for the radical cations the trans preference is even slightly more pronounced (3.6 kcal mol^{-1}).

The initial step for the reaction between ethene, **1**, and the *trans*-butadiene radical cation, **11**, is the formation of an ion−molecule complex, **12**, in which the ethene molecule is coordinated to a terminal carbon atom of the *trans*-butadiene cation (Figure 4). The type of interaction is analogous to that of the complex, **3** (involving *cis*-butadiene). The ethene moiety has a total positive charge of 0.22, and the positive spin density at C4 is reduced significantly (to 0.25) compared to isolated **11** (0.71). The stabilization energy of **12** is 6.2 kcal mol^{-1} which is slightly less than for **3** (6.6 kcal mol^{-1}). There is essentially no activation barrier for C4−C5 bond formation through transition structure **TS-12/13** (−0.1 kcal mol^{-1} vs **12**; ΔG^{298} is +0.5 kcal mol^{-1}) in analogy to the addition of ethene to *cis*-butadiene radical cation (via **TS-3/4**). The addition step from the complex **12** to the distonic intermediate **13** is exothermic by 2.0 kcal mol^{-1}. As was found for the cis route, rotation around the C4−C5 bond (via **TS-13/14**) can lead to C3−C6 bond formation with a very low barrier (1.8 kcal mol^{-1}) to give the vinylcyclobutane structure **14**. The same considerations as for **10** apply to **14**: The C3−C6 bond is considerably elongated (to 1.725 Å) due to strong interaction with the π-system at C1−C2. The CH_2 groups at C4 and C6 can exchange their chemical environment very easily through the C_s symmetry transition structure **TS-14/14** which is only 1.4 kcal mol^{-1} higher in energy than **14**. Hence, ethene can exchange terminal methylene groups with both *cis*- and *trans*-butadiene radical cations in the gas phase very easily ($\Delta G^{298\neq} = 4.4$ kcal mol^{-1} for *trans*- and 3.5 kcal mol^{-1} for *cis*-butadiene radical cation).

In the vinyl cyclobutane radical cation **14** with the vinyl group in an exo position, no rearrangement to a six-membered ring (analogous to **10** → **6**) may occur because this would generate a trans double bond (C2−C3) in a six-membered ring, causing too much strain. Formation of **6** is only possible after the vinyl group changes from the exo (**14**) to the endo position (**10**) through rotation about the C2−C3 bond. In the corresponding transition structure, **TS-10/14**, no hyperconjugative interaction between the C3−C6 single and the C1−C2 double bond is possible because of the unfavorable orientation of both. As a consequence, the C3−C6 distance is shortened to that of a normal C−C single bond (1.558 Å), and the C1−C2 and C2−C3 distances are somewhat longer compared to **14** (see Figure 4). Despite the loss of the hyperconjugative stabilization in the transition structure, the C−C rotational barrier involved is only 5.0 kcal mol^{-1} ($\Delta E^{0\neq}$ relative to **14**). The transition-state **TS-10/14** is not higher in energy than **13**. This means the cis (Path C, Chart 3) and the trans routes (Path D, Chart 4) are connected via **TS-10/14** with no extra barrier and **6** can be formed from **1** + **11** as easily as from **1** + **2** through a radical cation vinylcyclobutane/cyclohexene rearrangement. In **TS-10/14** a C1−C2 π- electron is missing; that is, the "hole" is located in the C1−C2 π-bond. The analogous transition state, **TS-10/14***, where the C1−C2 π-bond is intact and the hole is located in the C3−C6 σ-bond, is 17 kcal mol^{-1} higher in energy than **TS-10/14** at UHF/6-31G* and was not optimized at higher levels of theory. The preference for **TS-10/14** can be explained by

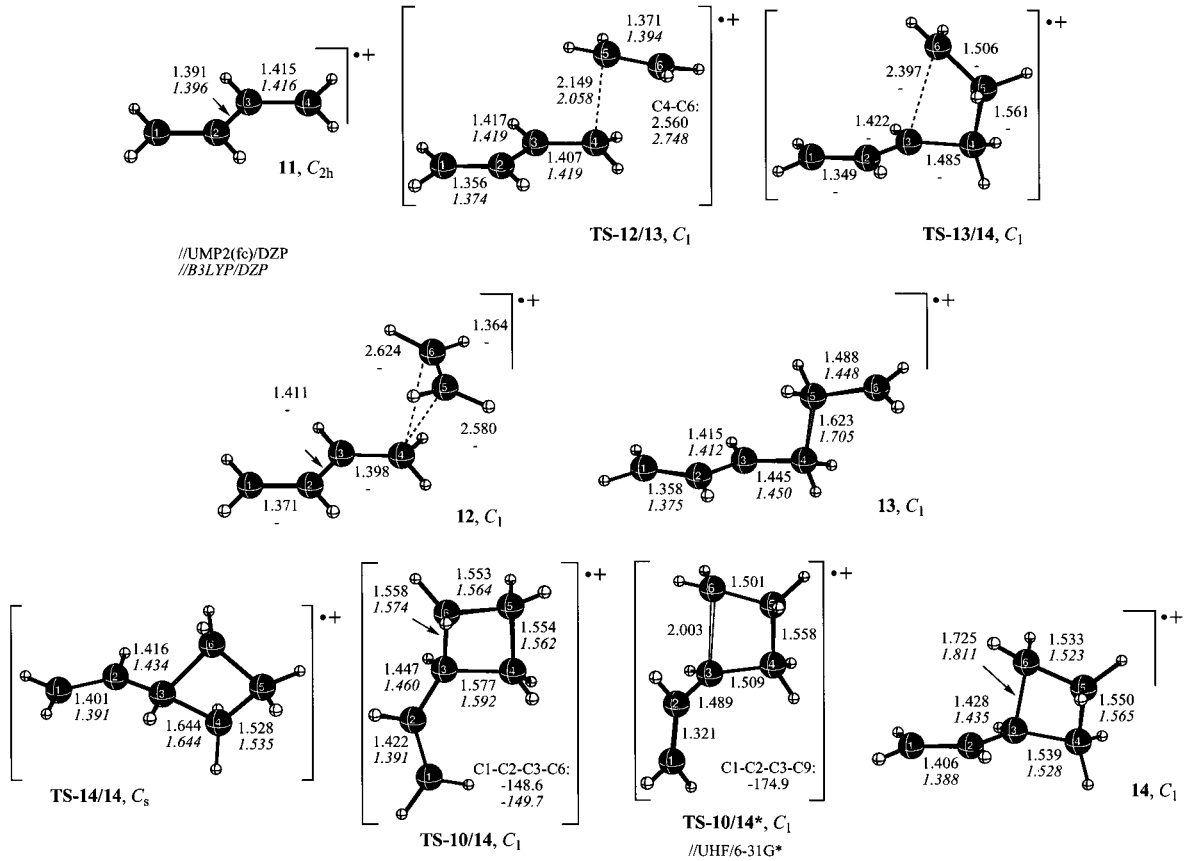

Figure 4. Optimized $[C_6H_{10}]^{\bullet+}$ geometries for path D: the addition of ethene, **1**, and *trans*-butadiene radical cation, **11**, to give the cyclohexene radical cation, **6**.

Chart 4

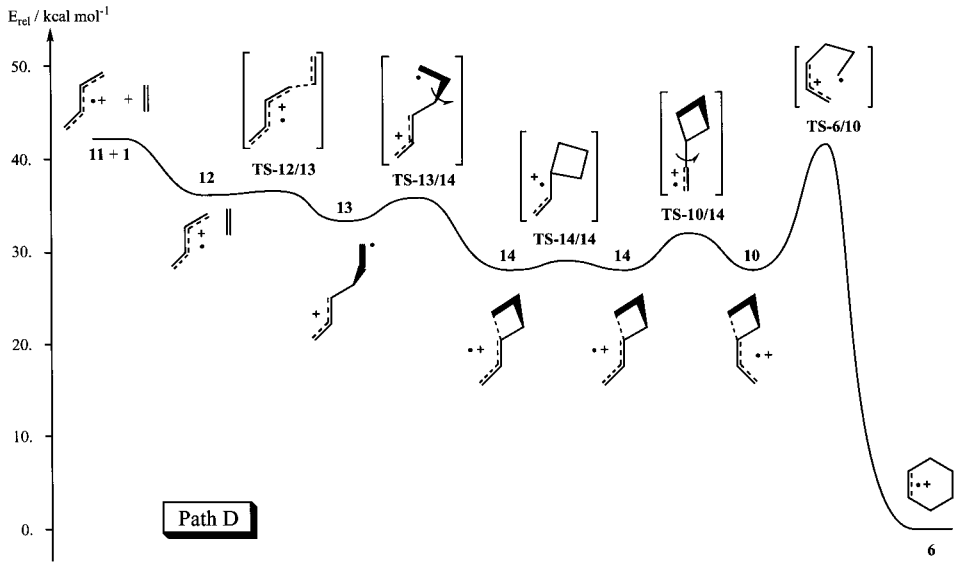

the energy difference of the σ- and the π-MO (in the neutral molecule) where one electron is missing from.

While cis/trans isomerization for neutral 1,3-butadiene is essentially a rotation around a single bond with a low barrier of ~3 kcal mol^{-1},[41] the missing electron from a C2−C3 antibonding orbital causes a much higher barrier in the radical cation case. Sastry et al. computed a 24.9 kcal mol^{-1} ($\Delta E^{0\neq}$; $\Delta H^{298\neq} = 22.4$ kcal mol^{-1}) barrier for the cis/trans isomerization of butadiene radical cation.[42] As evident from the results presented above, this process can be promoted by an ethene molecule: The reaction sequence **1** + **2** → **10** → **14** → **1** + **11** requires an activation of only 3.5 kcal mol^{-1} (ΔG^{298}). This sequence, however, includes exchange of terminal methylene groups between ethene, **1**, and *cis*-, **2**, or *trans*-butadiene radical cation, **11**, because of the low lying transition structures **TS-10/10** and **TS-14/14**.

(41) Murcko, M. A.; Castejon, H.; Wiberg, K. B. *J. Phys. Chem.* **1996**, *100*, 16162.

(42) Sastry, G. N.; Bally, T.; Hrouda, V.; Cársky, P. *J. Am. Chem. Soc.* **1998**, *120*, 9323.

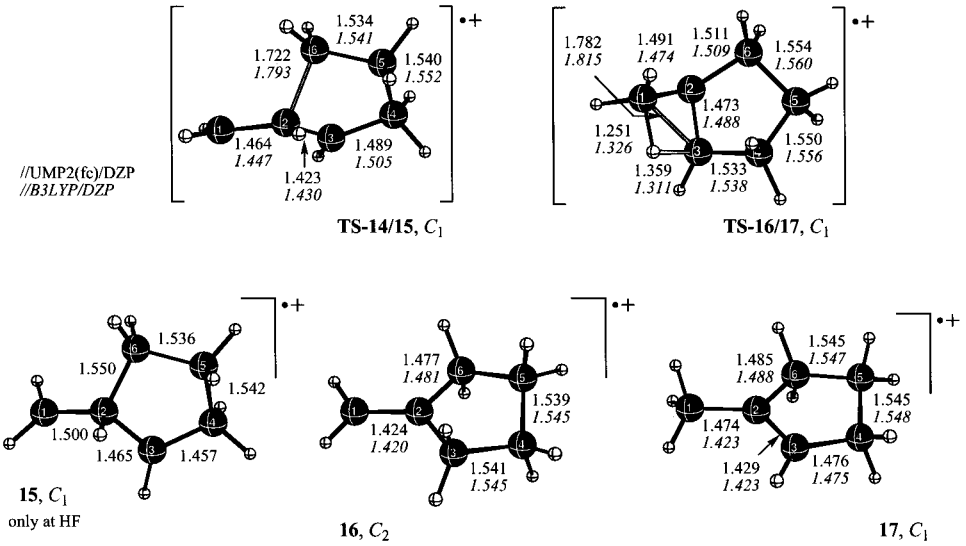

Figure 5. Optimized $[C_6H_{10}]^{\bullet+}$ geometries important in the reaction between ethene, **1**, to *trans*-butadiene radical cation, **11**, to give a five-membered ring product (path E).

V. Path E: Ring Expansion to Five-Membered Ring. Although no 1,3-alkyl shift is possible in **14** for steric reasons, ring expansion to a five-membered ring may occur by a 1,2-alkyl shift. This process generates two nonadjacent centers C1 and C3, one of which carries the spin (radical center) and the other which carries the charge (carbo cation center). Inspection of charges and spin densities computed for transition structure **TS-14/15** reveals that the 1,2-alkyl shift locates the unpaired electron onto C1 while C3 becomes the cation center. The latter has a preference for the bisalkylated C3 position. Following the IRC at UHF/3-21G leads to structure **15** which we could only locate at the SCF level (UHF/6-31G*). Refinement of the structure with correlated methods converged directly to **16** in which the hydrogen atom has migrated from C2 to C3 (Figure 5). This process not only moves the cationic center from a secondary to a tertiary position but also brings it next to the C1 radical center allowing for a one-electron π-bond. Hence, the methylenecyclopentane radical cation, **16**, is considerably more stable (24.5 kcal mol^{-1}) than the distonic **15** (//UHF/6-31G*). The fact that we could not locate a minimum for **15** at higher levels of theory suggests that the 1,2-alkyl (from **14** to **15**) and the 1,2-hydrogen shift (from **15** to **16**) might actually be coupled processes without a stationary point **15** in between. If **15** is really a stationary point, the barrier for the hydrogen shift should be vanishingly small. 1,2-H shifts can occur without barrier in carbocations. The transition-state **TS-14/15** for the formation of a five-membered ring requires a 6.3 kcal mol^{-1} activation (relative to **14**) and hence is only slightly less stable (by 1.3 kcal mol^{-1}) than **TS-10/14**, which connects **14** to path C leading to the cyclohexene radical cation, **6**. It is also only slightly (0.8 kcal mol^{-1}) higher in energy than the complex **12** on the ΔG^{298} surface.

Even more stable (by 10.6 kcal mol^{-1}) than **16** is the 1-methyl cyclopentene radical cation **17** with the oxidized double bond in the ring, which is the most stable $[C_6H_{10}]^{\bullet+}$ isomer we found. Isomer **17** could be generated from **15** by migration of a hydrogen atom from C2 to C1, but a 1,2-hydride shift from C2 to the cationic C3 seems preferred not only for electronic but also for steric reasons. The C2−H bond is oriented approximately parallel to the empty p-orbital at C2 (H−C2−C3−H = 81.3°) and is more or less perpendicular to the singly occupied p-orbital at C1 (H−C2−C1−H = −18.2°). A 1,3-H shift connects **16** to **17** and involves **TS-16/17** which is 42.2 kcal mol^{-1} higher in energy than **16**.

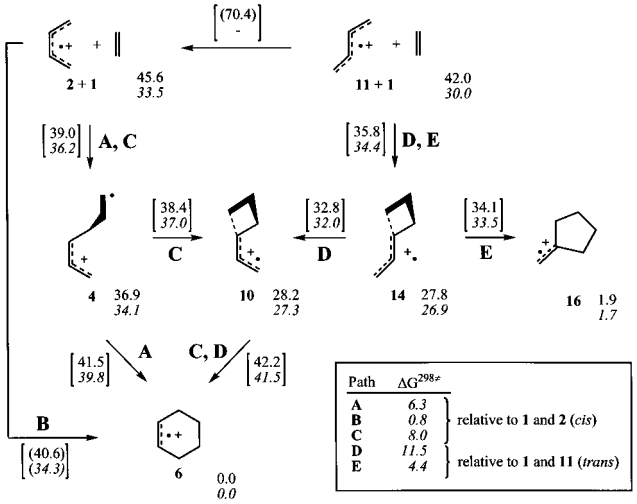

Figure 6. Relative energies (kcal mol^{-1}; $\Delta E°$ and ΔG^{298} in italics) of some $[C_6H_{10}]^{\bullet+}$ minimum structures and of the highest transition structures (in brackets) along reaction paths A−E. Values for path B have been interpolated from single-point calculations for UHF/6-31G* geometries. The barrier for cis/trans isomerization of butadiene radical cation is taken from ref 42.

Conclusions

Several reactions on the $[C_6H_{10}]^{\bullet+}$ potential energy surface (paths A−E) have been investigated computationally (compare Figure 6).

At 0 K, the addition of ethene, **1**, to the *cis*-butadiene radical cation, **2**, can give an open chain distonic intermediate, **4**, with no barrier and an exothermicity of 8.7 kcal mol^{-1}. At 298 K we find a change in free Gibbs energy (ΔG^{298}) of +0.6 kcal mol^{-1} and a small barrier of 2.7 kcal mol^{-1}. The stepwise cycloaddition to give the cyclohexene radical cation, **6**, by way of three intermediates (**3**, **4**, and **5**, path A) requires a total activation of 6.3 kcal mol^{-1} (ΔG^{298}) and has an energy change of −33.5 kcal mol^{-1} ($\Delta E° = -45.6$ kcal mol^{-1}). An alternative, direct addition (path B) was characterized at the HF/6-31G* level as stepwise, but the intermediate minimum and transition

structures could not be refined at electron-correlated levels as optimizations converged to different stationary points. Single-point computations on the stationary points suggest that this pathway might be a concerted, highly asynchronous addition with no or a very small activation barrier.

Ring closure of the open chain distonic intermediate **4** to a vinyl cyclobutane radical cation, **10**, requires even less activation (1.5 kcal mol^{-1}, $\Delta E^{0\neq}$) than isomerization to **6** via path A (4.6 kcal mol^{-1}). Isomer **10** has a C_1 structure but a C_s-symmetric transition structure, **TS-10/10**, is only 3.2 kcal mol^{-1} higher in energy. This finding explains the experimental observation that **1** and **2** exchange terminal methylene groups in the gas phase.[23] The activation energy of 48.6 kcal mol^{-1} for the neutral vinyl cyclobutane/cyclohexene rearrangement[36] is lowered to 14.0 kcal mol^{-1} for the radical cations. This indirect route (path C) leading also to the Diels−Alder product, **6**, has a barrier ($\Delta G^{298\neq}$) only 1.7 kcal mol^{-1} higher than path A (1.0 kcal mol^{-1} for $\Delta E^{0\neq}$).

The high barrier for cis/trans isomerization of the butadiene radical cation ($\Delta E^{0\neq}$ = 24.9 kcal mol^{-1}, $\Delta H^{298\neq}$ = 22.4 kcal mol^{-1})[42] can be reduced to 3.5 kcal mol^{-1} ($\Delta G^{298\neq}$; no barrier for $\Delta E°$) involving an ethene molecule: The latter adds to *trans*-butadiene radical cation **11** to give open chain **13**, with effectively no barrier. Intermediate **13** cyclizes readily to the vinyl cyclobutane radical cation for which the exo/endo rotational transition state, **TS-10/14**, is low in energy ($\Delta E^{0\neq}$ = 5.0 kcal mol^{-1}). Therefore, **11** + **1** can also form the Diels−Alder product (cyclohexene radical cation, **6**, path D) through the same barrier determining the transition structure for the vinyl cyclobutane/cyclohexene rearrangement, **TS-4/10**, as with *cis*-butadiene radical cation in path C.

However, the alternative ring expansion of the *exo*-vinylcyclobutadiene radical cation, **14**, to a five-membered ring (path E, Chart 5) is disfavored by only 1.3 kcal mol^{-1}.

The reaction of ethene with butadiene radical cation under low-pressure conditions in the gas phase does not produce cyclohexene radical cations because addition products cannot be deactivated. The gas-phase reaction is further elucidated by pathways reported in another paper.[43] Further work should clarify the relative influence of different substituents onto different pathways which were found to have activation barriers in a narrow energy range.

Chart 5

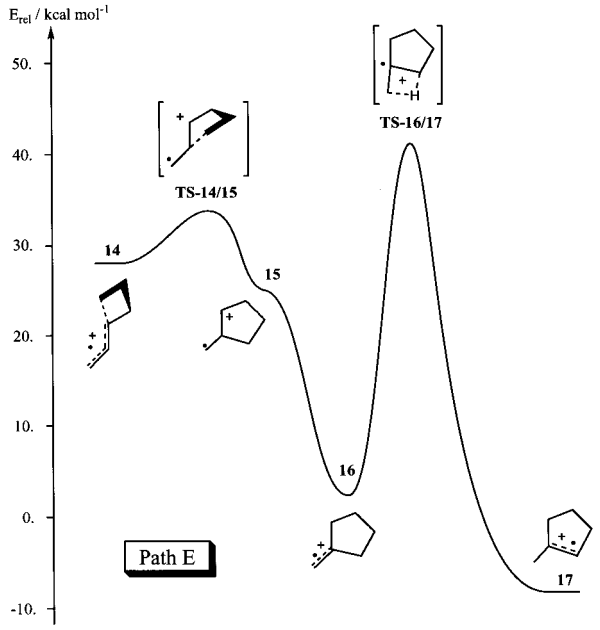

Acknowledgment. This research was supported by the U.S. Department of Energy, Office of Basic Energy Sciences, Fundamental Interactions Branch, Grant No. DOE-FG02-97ER14748. M.H. gratefully acknowledges a postdoctoral fellowship by the Deutscher Akademischer Austauschdienst (DAAD). We thank Professor Wiest for a preprint of ref 25.

Supporting Information Available: List of optimized Cartesian coordinates of $[C_6H_{10}]^{\bullet+}$ stationary points discussed in this work. Absolute energies at the highest level of geometry optimization and from CCSD(T)/DZP single energy point calculations are also included. This material is available free of charge via the Internet at http://pubs.acs.org.

JA983338Q

(43) Hofmann, M.; Schaefer, H. F. *J. Phys. Chem.*, submitted for publication.